Chapter 11
Photochromic Organometallics: Redox-Active Iron and Ruthenium Complexes with Photochromic DTE Ligand

Takashi Koike and Munetaka Akita

Abstract This chapter focuses on our works in the area of "photochromic organometallics" with a ***M***–C (***M***: redox-active metal fragments, C: carbon atom in the photochromic unit = dithienylethene (DTE)) bond. Smart molecular systems, which are designed to bring appropriate functions in response to change of the environment, are important foundations for the development of intelligent materials. Chromic molecules can recognize external stimuli so as to trigger chemical functions required for smart chemical systems. Combination with metal components, which exhibit unique properties such as redox and photophysical properties and catalysis, should lead to more sophisticated systems. In particular, photochromic molecules with metal fragments can provide an attractive molecular system driven by light. The first part is related to photoswitchable molecular wires. The second part deals with dual stimuli-responsive system, i.e., photo- and electrochromic organometallics. The use of dithienylethene, a representative photochromic molecule, is a key for unique chemical systems in this chapter.

Keywords Dithienylethene • Dual chromism • Electrochromism • Organometallic molecular wire • Photochromism

11.1 Introduction

Stimuli–responsive systems are essential components of smart chemical systems [1]. Stimuli–responsive systems can recognize changes of the environment so as to trigger a chemical function required for the smart chemical system. Many kinds of organic and inorganic stimuli–responsive systems have been developed so far.

T. Koike • M. Akita (✉)
Chemical Resources Laboratory, Tokyo Institute of Technology,
Nagatsuta, Midori-ku, Yokohama 226-8503, Japan
e-mail: koike.t.ad@m.titech.ac.jp; makita@res.titech.ac.jp

M. Irie et al. (eds.), *New Frontiers in Photochromism*,
DOI 10.1007/978-4-431-54291-9_11,

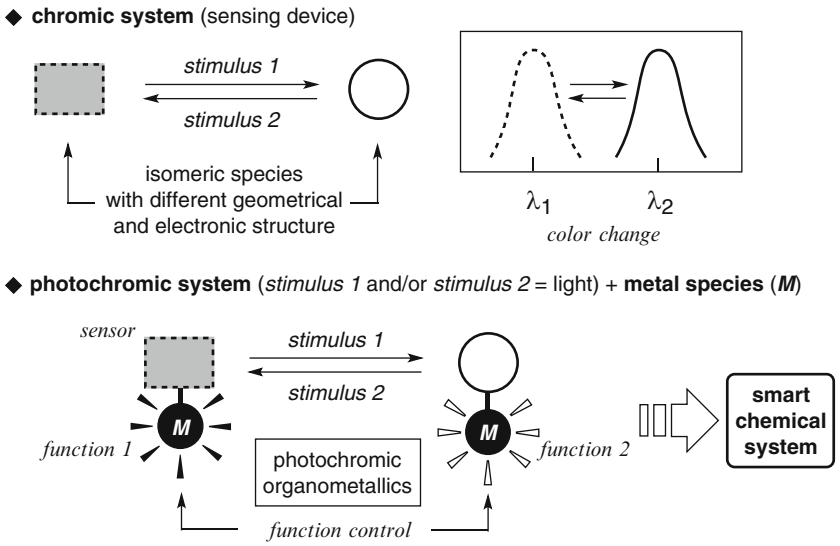

Fig. 11.1 Photochromic organometallics: combination of organic photochromic unit with metal species

Among them much attention has been focused on chromic systems [2]. Chromism is defined as a transformation of a chemical species between two forms by application of a stimulus, where the two forms have different absorption spectra, i.e., different colors, and the process is often reversible (Fig. 11.1).

The color change results from a change of the electronic structure of the chromic molecule (usually π-conjugated system), which is often associated with a change of the geometrical structure of the molecule. Combination of such chromic systems with other chemical systems should lead to the development of more sophisticated stimuli–responsive systems. One way is the combination of chromic π-conjugated organic fragments with metal species, which exhibit unique features such as redox properties, photophysical properties, and catalysis. There are many kinds of chromism, such as photo-, thermo-, iono-, halo-, electro-, solvato-, vapo-, and mechanochromism [2]. Herein photochromic system with metal complexes will be focused on, in particular, in which the photochromic unit is 1,2-dithienylethenes (DTE) [3, 4]. Over the past 10 years, photochromic metal complexes featuring other photochromes such as azobenzene, spiropyran, spirooxazine, benzopyran, and dimethyldihydropyrene derivatives have been developed from the viewpoint of modulation of photochromism or photoregulation of the redox, optical, and magnetic properties of metal units [5–10]. In addition, metal complexes themselves can also show photochromic properties usually via linkage isomerization of ligands [11]. In contrast to them, "photochromic organometallics" in this chapter refers to the DTE metal complexes, ***M***–DTE–***M*** or ***M***–DTE (***M***: redox-active metal fragments), with a ***M***–C bond. This molecular design of *photochromic organometallics* provides a promising way for creation of metal complexes with photochromic properties.

11.2 Photoswitchable Organometallic Molecular Wire

11.2.1 Introduction

Molecular electronics are regarded as one of the promising ways for miniaturization of electronic circuits leading to highly integrated electronic systems [12–25]. In order to build up molecular circuits, many molecular components such as wires, switches, transistors, and logic gates should be developed and assembled. The polyynediyldimetal complexes, ***M***–$(C{\equiv}C)_n$–***M*** (***M***: redox-active metal fragments), with a wirelike appearance are expected to display properties applicable to molecular wires [26–30], because the d-orbitals of the metal fragments at the termini may interact with each other through the π-conjugated $(C{\equiv}C)_n$ rod. For efficient communication between the two metal centers, the properties of the metal fragments must be best tuned [31–41]. Molecular electronics, however, are still in their infancy. Other molecular components need to be synthesized and their performance should be assessed [42]. Thus, we carried out the synthesis of switching systems.

11.2.2 1st Generation Dinuclear Iron and Ruthenium Complexes with Dithienylethene Ligand

Dithienylethene (DTE) has been chosen as the switching mechanism. The family of DTE is one of the versatile photochromic systems developed by Prof. Irie (Fig. 11.2) [3, 4]. Their photochromism is based on the reversible photochemical cyclization–cycloreversion processes between the open 1,3,5-hexatriene skeleton and the closed cyclohexadiene skeleton in the central part, and the forward and backward processes are triggered by UV and visible light irradiation, respectively. It is notable that the double bonds in the closed isomer **C** are fully conjugated, whereas the open isomer **O** contains cross conjugation at the thiophene–cyclopentene junctions. This dramatic structural change causes the striking color change (**O**: pale-colored, **C**: deep-colored), and DTE is superior to other photochromic systems with respect to many aspects such as quick response, fatigue resistance, and facile control of the photophysical properties (e.g., λ_{max}). If metal fragments are attached to the 5- and 5′-positions of the thiophene rings, the communication between the two metal centers through the DTE bridge may be switched.

Taking into account for the facile access to the acetylide complex-type skeleton, the DTE/Fe system with the C≡C linkers, *Fe*–C≡C–DTE–C≡C–*Fe* (*Fe* = $(\eta^5\text{–}C_5Me_5)$Fe(dppe), and dppe = $Ph_2PCH_2CH_2PPh_2$) (**1Fe*O**), was designed and readily synthesized from the corresponding 1-alkyne (Fig. 11.3) [43]. For the open isomer **1Fe*O** characterized by crystallographic methods, it is worthy of note that the DTE moiety

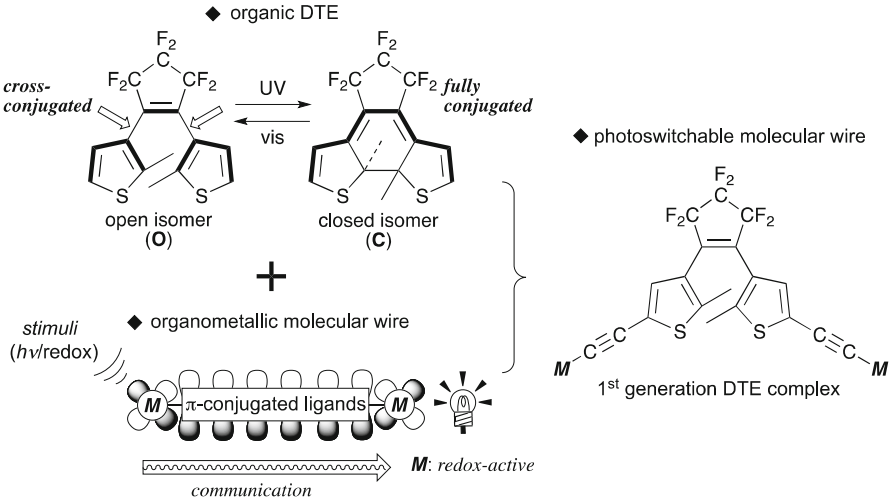

Fig. 11.2 Photoswitchable organometallic molecular wire (1st generation DTE complex)

adopts an antiparallel conformation suitable for photocyclization, i.e., the Fe groups bulkier than the central DTE part do not significantly affect the conformation of the central part in the ground state (Fig. 11.3a). The organometallic DTE derivative **1Fe*O** underwent photocyclization upon UV irradiation, in a manner similar to organic counterparts, to be converted to the closed isomer **1Fe*C**. A visible absorption at 774 nm grew progressively and reached a photostationary state with the composition of **1Fe*O/1Fe*C** = 10/90 in C_6D_6 (Fig. 11.3b). Subsequent visible light irradiation of the equilibrated mixture regenerated **1Fe*O** quantitatively. After ten photochemical cyclization–cycloreversion cycles, no noticeable deterioration was detected. Switching factor (SF) can be evaluated by comparison of wirelike performance of **1Fe*O** with that of **1Fe*C**. In general, wirelike performance of organometallic molecular wires is estimated on the basis of K_C value (comproportionation constant) obtained by electrochemical analysis. Wirelike behavior is attributed to the stability of monocationic species, that is, the mixed-valence (MV) complex. The K_C value is derived from the potential difference between the two-redox process (ΔE) according to the equation, $K_C = \exp(\Delta E \times F/RT)$ (F: Faraday constant (9.65×10^4 C mol^{-1}), R: gas constant (8.31 J K^{-1} mol^{-1}), T: temperature (K)), and represents the thermodynamic stability of the mixed-valence monocationic species against non-mixed-valence ones, indicating that the extent of delocalization of the hole over the bridging part (Fig. 11.4).

The two isomers (**1Fe*O** and **1Fe*C**) isolated by repeated recrystallization were subjected to electrochemical measurements to determine the K_C values. For the open isomer **1Fe*O**, as can be seen from the CV trace, a slightly broad single redox wave was observed indicating very weak interaction between the two metal centers with $K_C = 13$ as analyzed by simulation of the CV trace (Fig. 11.3c) and

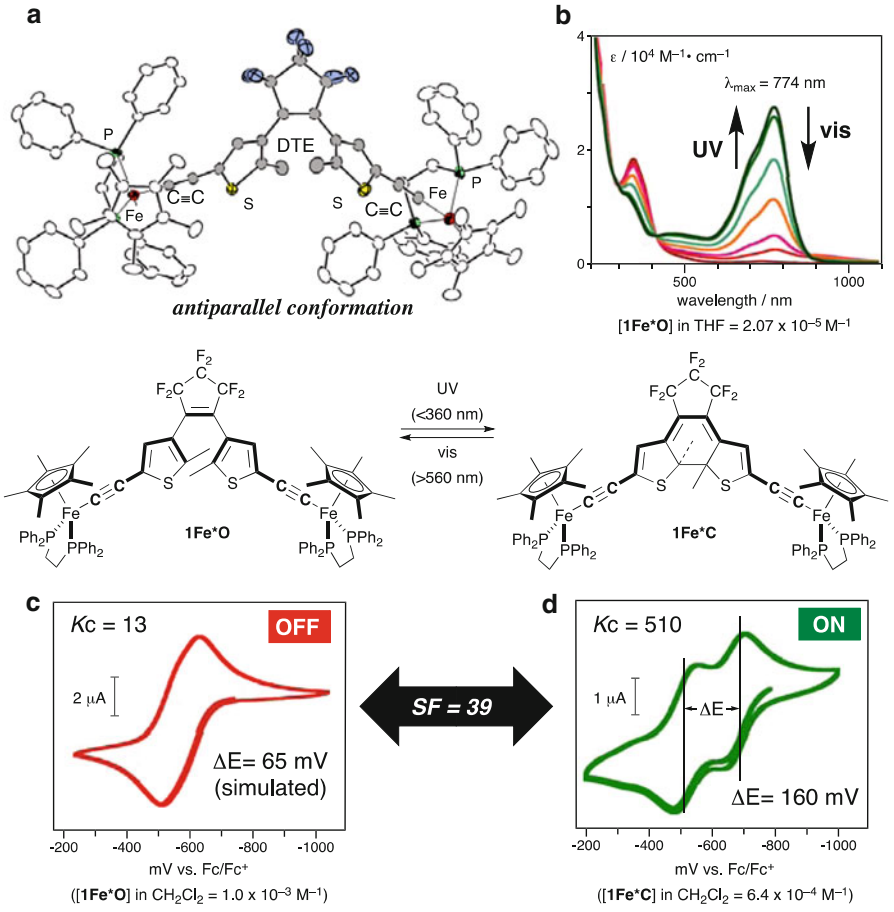

Fig. 11.3 (**a**) Molecular structure of **1Fe*O**; (**b**) UV–vis spectra for photochromism of **1Fe***; (**c**) CV trace for **1Fe*O**; (**d**) CV trace for **1Fe*C**

deconvolution analysis of a differential pulse voltammetry (DPV) trace. In sharp contrast, the closed isomer **1Fe*C** showed two separated redox waves (Fig. 11.3d). From the separation ($\Delta E = 160$ mV), the K_C value was determined to be 510, which is significantly larger than that of the open isomer. As a result, the switching factor, SF = K_C (closed)/K_C (open), turned out to be calculated at 39. It is clear that the present iron DTE complex **1Fe*** is an excellent photoswitchable molecular wire [44].

The isoelectronic complexes, *Ru*–C≡C–DTE–C≡C–*Ru* (*Ru* = (η^5–C_5Me_5)Ru(dppe)) (**1Ru*O**), were also prepared and tested for photochromic behavior and switching factor [45]. It should be noted that photochromic performance is significantly improved (**1Ru*C** was formed quantitatively under UV irradiation). Quantum yields (in toluene) were determined to be 0.0021 (**1Fe*O**; irradiated at 366 nm) and 0.38 (**1Ru*O**;

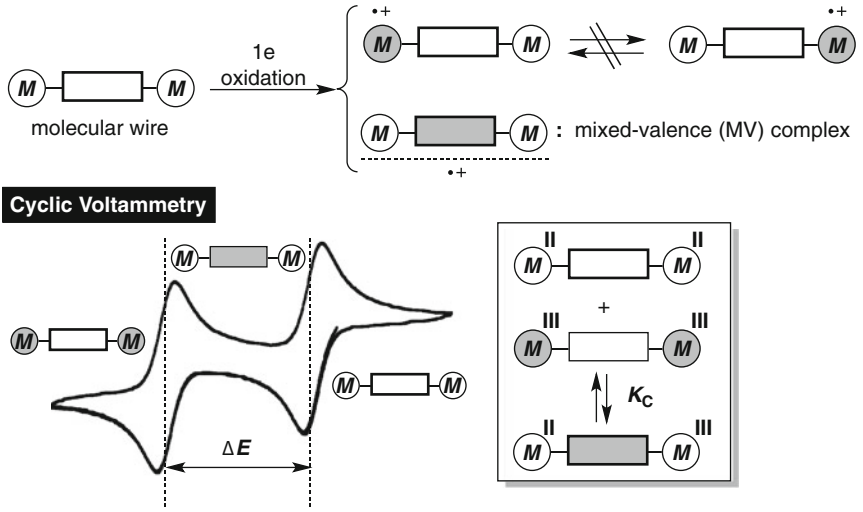

Fig. 11.4 Evaluation for organometallic molecular wires based on electrochemical analysis

irradiated at 366 nm) for the ring-closing processes and 0.00018 (**1Fe*C**; irradiated at λ_{max} of **1Fe*C** (768 nm)) and 0.00044 (**1Ru*C**; irradiated at λ_{max} of **1Ru*C** (710 nm)) for the ring-opening processes. Note that although the ring-closing quantum yield of **1Ru*O** is comparable to that of the diphenyl derivative, C_6H_5–DTE–C_6H_5 **5** (1,2-di(2-methyl-5-phenylthien-3-yl)-3,3,4,4,5,5-hexafluorocyclopentene), (0.59 for ring closure and 0.013 for ring-opening in hexane) [46], the ring-opening quantum yields are significantly even smaller than the rather small quantum yield for the ring-opening process of **5**. On the other hand, switching performance of **1Ru*** (SF = 4) is inferior to that of **1Fe***. These results show that the structures of metal fragments strongly affect photochromic properties as well as redox properties.

11.3 Dual Photo- and Electrochromic Organometallics

11.3.1 Introduction

To gain further insight into the effect of metal fragments on photochromic behavior, we designed a new series of 2nd generation DTE complexes without acetylene linkers, ***M***–DTE–***M*** (***M*** = (η^5–C_5R_5)ML_2, M = Fe, Ru; L = CO, phosphine), which redox-active metal fragments are directly σ-bonded to the thiophene rings at the 5,5′-positions (Fig. 11.5 and Table 11.1).

In addition, computational analysis was conducted to investigate the photochemical process in detail. Time-dependent DFT (TDDFT) calculations suggested that the photocyclization proceeds via triplet excited state, which is a different reaction pathway from the proposed process in the photocyclization of normal organic DTE.

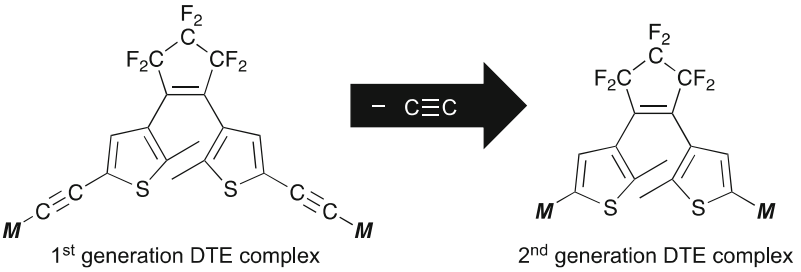

Fig. 11.5 Molecular design of 2nd generation DTE complex

Table 11.1 Photochromic behavior of DTE complexes (**1**–**4**)

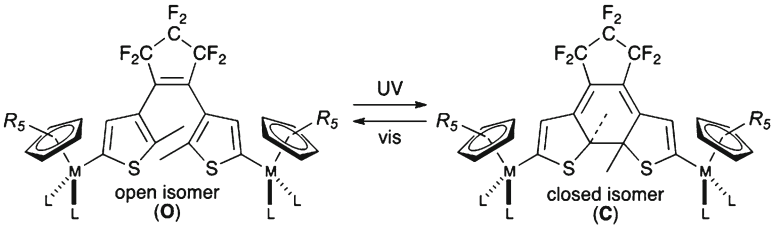

Complex	***M*** **((η⁵–C_5R_5)ML_2)**	**O/C**[a]	Ring closure[b] (time/min)	Ring opening[b] (time/min)	λ_{max}/nm of **C** (color)	Recycl. (times)
1Fe*	C≡C–Cp*Fe(dppe)	10/90	80	90	774 (green)	95 % (6)
1Ru*	C≡C–Cp*Ru(dppe)	~0/~100	8	60	719 (green)	88 % (10)
2Fe	$CpFe(CO)_2$	61/39	16	4	560 (brown)	Decomp.
2Ru	$CpRu(CO)_2$	36/64	24	4	549 (brown)	50 % (5)
3Fe	$CpFe(CO)(PPh_3)$	90</<10	–	–	–	Decomp.
3Ru	$CpRu(CO)(PPh_3)$	30/70	30	8	584 (blue purple)	70 % (10)
4Fe′	Cp′Fe(dppe)	100/0	–	–	–	–
4Fe*	Cp*Fe(dppe)	100/0	–	–	–	–

[a]Isomer ratios at the photostationary states in C_6D_6 determined by ^1H NMR
[b]Monitoring 2.0×10^{-5} M in THF by UV–vis spectra

Furthermore, these "photochromic organometallics" exhibit ring-closing reaction triggered by 2e-oxidation, i.e., the present molecular system provides dual photo- and electrochromic system. Multi-stimuli–responsive systems can be key elements for the construction of molecular devices as well as smart chemical systems, because they are expected not only to simply work as a switch but also to be applicable to logic systems. Combination of a photoresponsive DTE unit with redox-active metal fragments has potentials to produce multi-stimuli–responsive systems and multi-chromism. We also developed the mononuclear DTE complexes, ***M***–DTE (***M*** = (η⁵–C_5H_5)ML_2, M = Fe, Ru; L = CO, phosphine), which express dual chromism in a manner different from dinuclear complexes.

11.3.2 2nd Generation Dinuclear Iron and Ruthenium Complexes with Dithienylethene Ligand

A series of 2nd generation DTE complexes, ***M***–DTE–***M*** (***M*** = (η^5–C_5H_5)Fe(CO)$_2$ (**2Fe**), (η^5–C_5H_5)Ru(CO)$_2$ (**2Ru**), (η^5–C_5H_5)Fe(CO)(PPh_3) (**3Fe**), (η^5–C_5H_5)Ru(CO)(PPh_3) (**3Ru**), (η^5–C_5H_4(Me))Fe(dppe) (**4Fe′**), and (η^5–C_5Me_5)Fe(dppe) (**4Fe***)), was prepared by (a) metalation of the lithiated DTE using the corresponding carbonyl metal halides, (η^5–C_5R_5)MX(CO)$_2$ (M/X=Fe/I and M/X=Ru/Cl), and (b) subsequent photochemical ligand exchange reactions. Some of the derivatives are characterized by single-crystal X-ray crystallography, which reveals the open structure with the antiparallel conformation of the two thiophene rings being suitable for photochemical ring closure [47, 48]. The obtained organometallic DTE complexes exhibit photochromic behavior but the performance turns out to be dependent on the attached metal fragments, as expected from above-mentioned results (Sect. 11.2.2). The photochromic behavior on the basis of UV–vis spectra and NMR data was summarized in Table 11.1.

Complexes **2Fe**, **2Ru**, and **3Ru** undergo the reversible photochemical interconversion, whereas the other complexes **3Fe**, **4Fe′**, and **4Fe*** are virtually inert with respect to the photochromism. Isomer ratios (**O/C**) at the photostationary states in C_6D_6 are estimated to be 61/39 for **2Fe**, 36/64 for **2Ru**, 91/9 for **3Fe**, and 30/70 for **3Ru**. Dependence of the photochromic performance can be estimated by the isomer ratios at the photostationary states as follows: metal: Ru > Fe; ligand: $(CO)_2$ > (CO)(PPh_3) ≈ dppe (for the iron complexes), $(CO)_2$ ≈ (CO)(PPh_3) (for the ruthenium complexes); and linker: C≡C (**1**) > none (**2**–**4**). Dependence on the metal will be discussed in the next Sect. 11.3.3 on the basis of theoretical analysis. It should be noted that conversion of **2Ru** and **3Ru** to the closed isomers **C** is incomplete, whereas the acetylide derivatives **1Ru*** are converted to the closed isomers almost quantitatively. The difference could be ascribed to the absorption ranges of the closed isomers. The envelope of the UV absorption of the open isomers **O** could be extended to the absorption ranges of **2RuC**–**3RuC** (550–600 nm) but not to that of **1Ru*C** (>700 nm) being in the far longer wavelength region. Stability (fatigue resistance) of the organometallic DTE complexes is dependent on the structure of the metal auxiliaries. For the stability, the following orders are noted: metal: Ru > Fe and ligand: (CO)(PPh_3) > $(CO)_2$. The stability appears to be limited by photochemical decarbonylation and, therefore, is dependent on the strength of back-donation to the CO ligands. The CpM(CO)(PPh_3) complexes **3** are more robust than the CpM$(CO)_2$ complexes **2**, and the ruthenium complexes are more stable than the iron derivatives. In accord with this consideration, any notable deterioration was not observed for the dppe complexes without a CO ligand, **4Fe′** and **4Fe***, although they did not show photochromic behavior.

Quantum yields for the ring-closing and ring-opening processes of a representative example **2Ru** in toluene were determined to be 0.22 (irradiated at 355 nm) and 0.011 (irradiated at λ_{max} of **2RuC** (549 nm)), respectively. For **2FeC**, the ring-opening quantum yield was determined to be 0.016 (irradiated at λ_{max} of **2FeC**(560 nm)), but determination of the ring-closing quantum yield was hampered by the

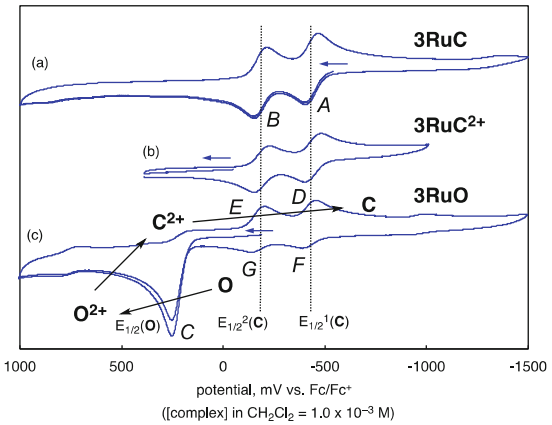

Fig. 11.6 CV traces for **3RuC**(a), **3RuC**$^{2+}$(b), and **3RuO**(c)

photochemical decomposition mentioned above proceeding at a rate comparable to that of the ring-closing process. It is notable that the ring-closing quantum yield of **2RuO** is in the same range of those of the organic diphenyl derivative, Ph-DTE-Ph **5**, (0.59 in hexane) and the ruthenium-acetylide complex **1Ru*O** (0.38) but significantly larger than that of **1Fe*O** (0.0021). On the other hand, the ring-opening quantum yields of **2FeC** and **2RuC** are virtually the same as that of **5** (0.013 in hexane) and even much larger than those of for **1Fe*C** (0.00018) and **1Ru*C** (0.00044). Thus, it turns out that photochemical reactivity of the ruthenium complexes is superior to that of the corresponding iron derivatives. The 2nd generation DTE complexes exhibit the photochromic properties in a manner similar to that of organic derivatives but the performance is dependent on the metal and ancillary ligands. With respect to central metal, it has similar results as those of 1st generation DTE complexes.

Electrochemical behavior turns out to also be dependent on the attached metal fragments. Behavior of the **2**- and **3**-series complexes is considerably different from that of the **4**-series dppe complexes. As a typical example, electrochemical behavior of **3Ru** is described in detail (Fig. 11.6). The closed isomer **3RuC** shows the reversible, two consecutive 1e-redox waves at −430 (*A*) and −174 mV (*B*) (vs. $[FeCp_2]/[FeCp_2]^+$; Fig. 11.6a). The CV trace for the open isomer **3RuO** (Fig. 11.6c) is totally different from that of **3RuC**. A 2e-oxidation wave is observed at 273 mV (*C*) but the corresponding reduction wave is not detected and, instead, two consecutive reduction waves are observed at −495 (*D*) and −217 mV (*E*). A subsequent anodic scan gives two oxidation waves (*F* and *G*) corresponding to the two reduction processes (*E* and *D*, respectively). These two redox processes observed at $E_{1/2}$ = −430 and −174 mV (*D*–*G*) are superimposable on those of the closed isomer **3RuC** (*A* and *B*) mentioned above. These results suggest that 2e-oxidation induces cyclization of the open isomer. Similar electrochemical behavior is observed for the open isomers of the ruthenium complex **2RuO** and the iron complexes **2FeO** and **3FeO**. In contrast to **2O** and **3O**, the dppe complexes **4Fe′O** and **4Fe*O** show two consecutive reversible 1e-redox waves when scanned in the range of −1,500 to 500 mV.

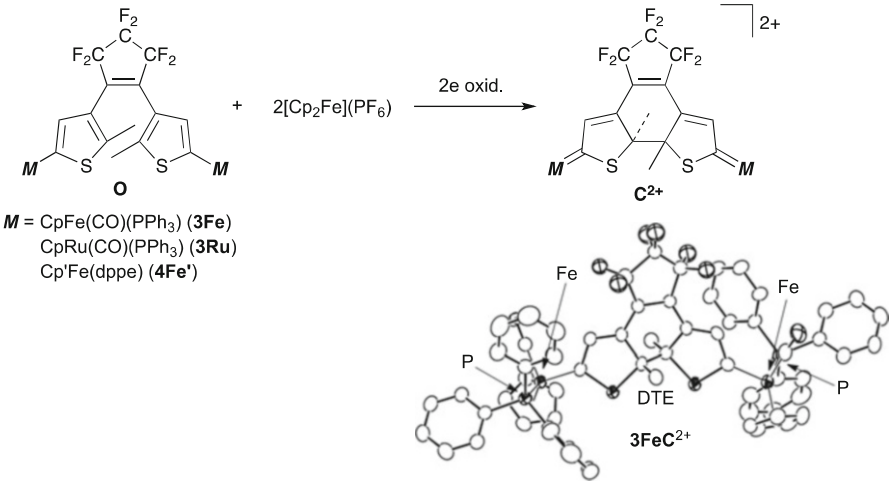

Fig. 11.7 Oxidative cyclization of **3FeO**, **3RuO**, and **4Fe′O** and ortep drawing of **3FeC**$^{2+}$

To confirm the chemical events taking place, chemical oxidation of the DTE complexes was conducted. Treatment of **3FeO**, **3RuO**, and **4Fe′O** with $[FeCp_2]PF_6$ (2 equiv.) gave the isolable, deep-green-colored diamagnetic dicationic closed species, [**3FeC**$^{2+}$]$(PF_6)_2$, [**3RuC**$^{2+}$]$(PF_6)_2$, and [**4Fe′C**$^{2+}$]$(PF_6)_2$, respectively (Fig. 11.7). Single-crystal X-ray crystallography of one of the stereoisomers of [**3FeC**$^{2+}$]$(PF_6)_2$ confirms (a) formation of a C–C single bond between the two thiophene rings at the 2- and 2′-positions (1.52(1) Å), (b) the double bond character of the Fe═C moieties (1.858(6) and 1.872(6) Å) substantially shorter than the Fe–C single bond, and (c) a change of the pattern of the bond alternation in accordance with the canonical form **C**$^{2+}$ depicted in Fig. 11.7. The CV trace for the dicationic species **3RuC**$^{2+}$ (Fig. 11.6b) identical to that of the neutral closed species (Fig. 11.6a) verifies that the two species contain the same closed carbon skeleton with different π-conjugated systems. It is significant that the Fe–phosphine complexes **3FeO** and **4Fe′O**, which do not undergo the photochemical ring closure, cyclize quantitatively upon the 2e-oxidation. As expected from the bond alternation pattern of **C**$^{2+}$, the dicationic closed isomers are so stable under daylight and do not undergo photochemical cycloreversion in contrast to the neutral closed isomers **C**. In addition, reduction of the dicationic closed species **C**$^{2+}$ by cobaltocene, $CoCp_2$, gave the corresponding neutral closed species **C**. For **2FeO** and **2RuO**, sequential in situ oxidation by CAN (cerium ammonium nitrate) and reduction with $CoCp_2$ at −78 °C afforded the neutral closed species **2C**, indicating occurrence of an analogous redox process. The cyclic voltammograms for complexes **2** similar to those of **3Ru** also suggested occurrence of analogous oxidative ring closure but the cationic carbene intermediate **2C**$^{2+}$ was too unstable to be isolated because of the lack of an electron-donating ligand (e.g., phosphine ligand) for stabilization of the electron-deficient Fischer-type carbene functional group [49, 50]. The dppe complexes **4Fe′O** and **4Fe*O** exhibit CV features different from those of **2** and **3** as mentioned above. The Cp′ complex **4Fe′O**

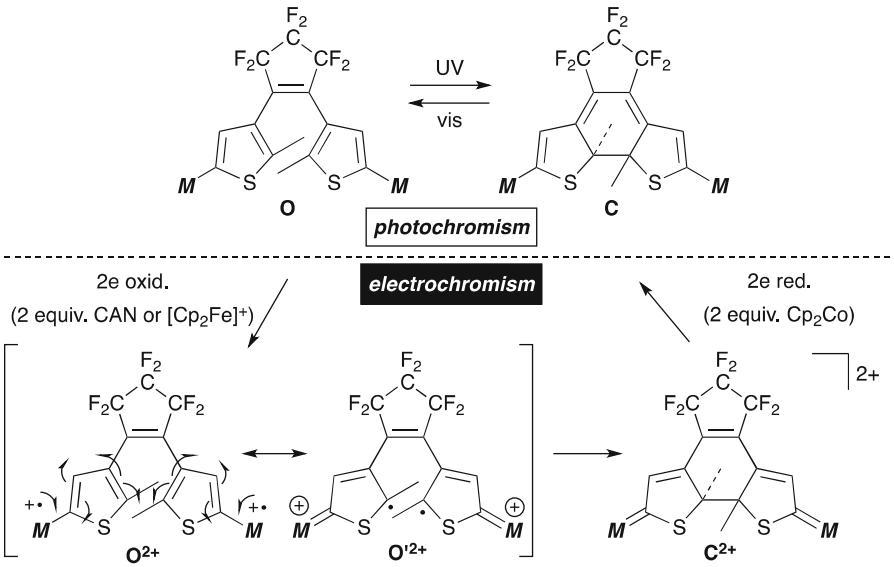

Fig. 11.8 Dual photo- and electrochromic behavior

underwent oxidative cyclization in a manner similar to **3Fe** and **3Ru** to give [**4Fe′C**$^{2+}$]$(PF_6)_2$, although reduction of the resultant dicationic species with $CoCp_2$ did not afford **4Fe′C** but a complicated mixture of products. On the other hand, 2e-oxidation of the Cp* complex **4Fe*** did not afford the cyclized product but the isolable, paramagnetic, open diradical species **4Fe*O**$^{2+}$, which shows the same CV features as those of **4Fe*O**.

The redox processes of the 2nd generation DTE complexes **2**–**4** can be interpreted in terms of the reaction sequence summarized in Fig. 11.8. The 2e-oxidation of **O** should give the dicationic diradical species **O**$^{2+}$. The radical centers in **O**$^{2+}$ should be delocalized over the thiophene rings in resonance with the thienyl radical form **O**$'^{2+}$, which undergoes radical coupling at the 2- and 2′-positions of the thiophene rings to give the closed diamagnetic species **C**$^{2+}$. Subsequent 2e-reduction gives the neutral closed isomer **C**. The lack of reduction waves for the oxidized, open dicationic species **O**$^{2+}$ (Fig. 11.6c) indicates that the ring closure (**O**$^{2+}$ → **C**$^{2+}$) proceeds at a rate faster than the time scale of the CV measurement. A further cathodic scan gives the two reduction waves for the generated, closed dicationic species **C**$^{2+}$, which are identical to those of the neutral closed isomer **C**. The ring closure of the Cp′Fe(dppe) complex **4Fe′** should follow an analogous reaction sequence but the different CV features could be ascribed to the different time scales for the CV measurement and the chemical oxidation. The electron-donating dppe ligand should stabilize the electron-deficient diradical species **O**$^{2+}$ to elongate its lifetime. As a result, the rate of the ring-closing process becomes slower than the CV time scale but substantial with respect to the time scale of the preparative experiment. Further introduction of the electron-donating Cp* ligand (**4Fe***) finally makes the diradical

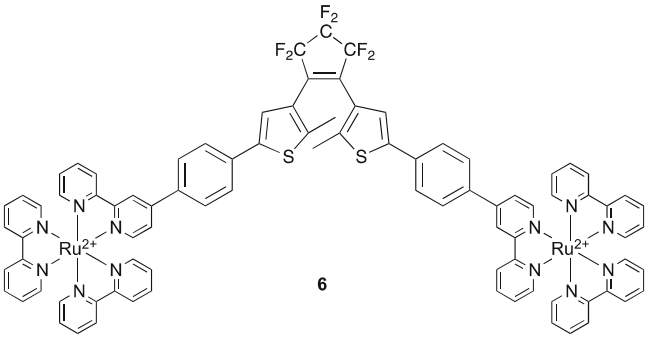

Fig. 11.9 A DTE complex with the $Ru(bpy)_3$ units **6**

intermediate **4Fe*O**$^{2+}$ stable so as not to undergo the cyclization. Our studies have been followed by a few related DTE–metal complexes with ring closure induced by oxidation [51, 52].

Thus, it has been revealed that the 2nd generation DTE complexes exhibit not only photochromism but also electrochromism, i.e., dual chromic behavior. Similar electrochromism is also observed in organic DTE system [53–59], however, the feature of the present "photochromic organometallics" is the involvement of isolable **C**$^{2+}$. The three colors (**C**, **O**, **C**$^{2+}$) can be expressed by a single molecule in response to different stimuli (light and redox).

11.3.3 Computational Analysis on Photochromism of Dithienylethenes with Metal Fragments

To gain further insight into the photochemical processes observed for the dinuclear DTE system, time-dependent DFT (TDDFT) analysis [60–63] was performed for singlet and triplet excited states of the $CpM(CO)(PMe_3)$ complexes **3#Fe** and **3#Ru** (simplified PMe_3-substituted analogues of **3Fe** and **3Ru**, respectively).

It has been established for organic DTE molecules that the ring closure occurs via the lowest singlet excited state (corresponding to S_9 for **3#Fe** in Fig. 11.10a) [64, 65]. By contrast, De Cola and her coworkers recently studied photophysical properties of a transition metal complex **6**, where the photochemically active $Ru(bpy)_3$ fragments were attached to DTE (Fig. 11.9), and proposed that the ring closure of **6** proceeds not only via the ligand(DTE)-centered singlet state but also via the ligand-centered triplet state resulting from energy transfer processes by way of the metal-based excited states [66]. Taking into account for these two extreme cases, we have carried out TDDFT analysis. To be explained is the following photocyclization tendency observed for the central metal: Ru > Fe.

Energy levels for Franck–Condon states for the two complexes are summarized in Fig. 11.10. Singlet and triplet states are denoted by bold lines and plain lines,

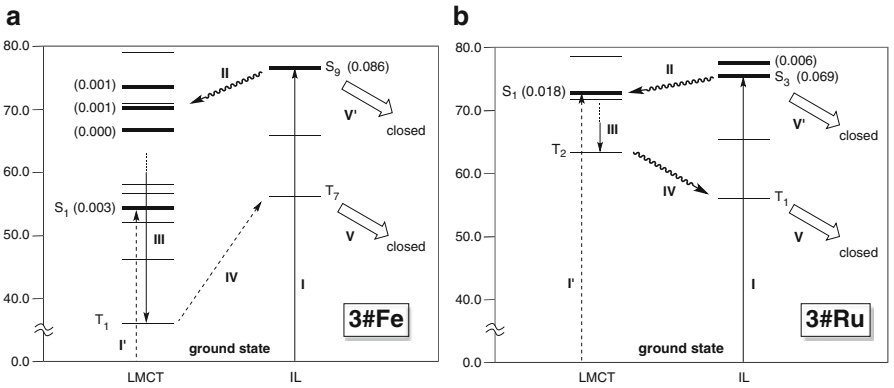

Fig. 11.10 Energy diagrams for Frank–Condon excited states of **3#Fe** (**a**) and **3#Ru** (**b**). *Bold lines*: singlet states; *plain lines*: triplet states

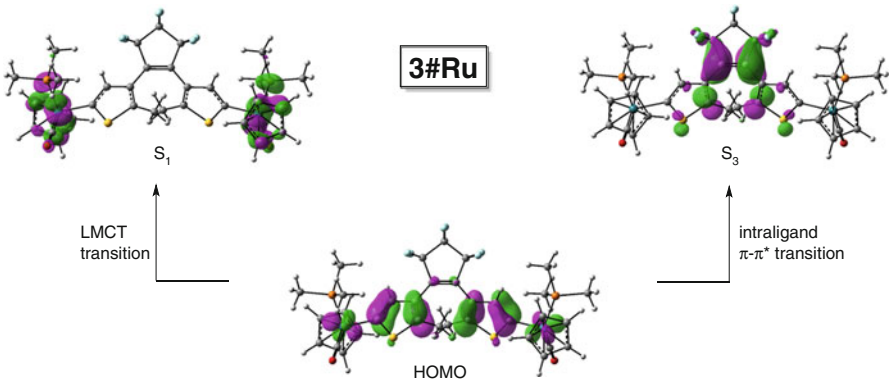

Fig. 11.11 HOMO and the lowest metal-(S_1) and ligand-based singlet excited states (S_3) for **3#Ru**

respectively, and labels for the excited states of higher energies are omitted for clarity. The excited states can be divided into two categories, LMCT and IL (intraligand). The excited states of the LMCT series are metal d-orbital-based, whereas those of the IL series are DTE-based, as can be seen, for example, from the S_1 and S_3 states of the CpRu(CO)(PMe_3) complex **3#Ru** (Fig. 11.11). In addition, the metal-based LMCT series orbitals contain antibonding combinations between the metal d-orbital and the ligand orbitals (Cp, CO, and PR_3). These features are common to these complexes discussed herein.

Let us consider the chemical processes of **3#Ru** (Fig. 11.10b). Irradiation causes excitation of a HOMO electron to singlet orbitals of higher energies. The S_1 state resulting from LMCT transition lies substantially lower in energy than the S_3 state resulting from IL transition, suggesting that the initial excitation may occur toward the S_1 state preferentially. The oscillator strength shown in parentheses, which

indicates relative transition probability, clearly demonstrates that the GS(S_0)→S_3 transition (**I**) is the most probable and major initial photochemical event; the oscillator strength for the GS→S_3 transition (0.069) is substantially larger than the negligible oscillator strength for other transitions (<0.018). The energy level of S_3 is in the UV region in accordance with the lack of a visible band for **3Ru**. Subsequent energy transfer to a LMCT excited state (**II**) followed by intersystem crossing and relaxation according to the Kasha's rule (**III**) leads to the lowest LMCT triplet state T_2. Further back energy transfer toward the DTE part leads to the lowest excited state T_1 with the significant DTE-based character (**IV**). Let us point out that the MO features for the DTE moiety in T_1 (MO is the same as that for S_3 depicted in Fig. 11.11), i.e., (a) antibonding combination of the p-orbitals of the C═C moiety in the cyclopentene ring, (b) π-bonding interactions at the thiophene–cyclopentene junctions, and (c) in-phase combination of the p-orbitals of the 2- and 2′-carbon atoms in the thiophene rings to be connected in the closed isomer, are reminiscent of the molecular orbital of a closed cyclohexadiene skeleton. These features tell us that the final ring-closing process from T_1 (**V**) is a likely process.

Then we examined the effects of the metal centers. For the iron analogue **3#Fe**, an energy diagram similar to that for **3#Ru** is obtained (Fig. 11.10a) but a significant difference is noted for the relative energy gap between the excited states associated with step **IV**. The DTE-based T_7 state lies significantly higher in energy than the lowest metal-based triplet state T_1 so that the final endothermic process **IV** is not viable and, as a result, the iron complex **3#Fe** eventually deactivates to the ground state without cyclization. The dependence of the efficiency of the photocyclization on the central metal (Ru > Fe) has been successfully interpreted in terms of the mechanism involving the crucial metal-to-DTE energy transfer step **IV**. The inertness of **3#Fe** reveals that the ring closure of the organometallic DTE compounds may proceed via triplet excited states, because, otherwise, photocyclization should occur directly via the initial singlet state (S_9) in a manner similar to organic derivatives. The inertness suggests that energy transfer from S_9 to LMCT triplet states is much faster than direct ring closure from S_9.

More recently, our collaborators, the group of Dr. Nakamura, reported on explanation for ancillary ligand effect on the photocyclization of **2Fe** and **3#Fe** [67]. However, the origin of the dependence on the metal fragment is still open to further discussion and investigation.

11.3.4 Mononuclear Iron and Ruthenium Complexes with Dithienylethene Ligand

A series of mononuclear DTE complexes, ***M***–DTE (***M*** = (η^5–C_5H_5)Fe$(CO)_2$ (**7Fe**), (η^5–C_5H_5)Ru$(CO)_2$ (**7Ru**), (η^5–C_5H_5)Fe$(CO)(PPh_3)$ (**8Fe**), (η^5–C_5H_5)Ru$(CO)(PPh_3)$ (**8Ru**), and (η^5–C_5H_4(Me))Fe(dppe) (**9Fe**)), was prepared in a manner similar to the synthesis of dinuclear complexes.

Table 11.2 Photochromic behavior of the mononuclear DTE complexes (**7**–**9**)

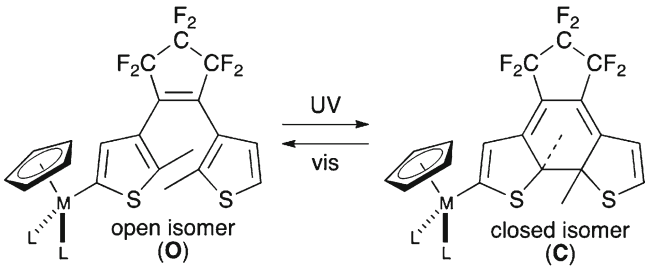

Complex	***M*** **((η⁵–C_5H_5)ML_2)**	**O/C**[a]	Ring closure[b] (time/min)	Ring opening[b] (time/min)	λ_{max}/nm of **C** (color)	Recycl. (times)
7Fe	$CpFe(CO)_2$	–	–	–	–	Decomp.
7Ru	$CpRu(CO)_2$	62/38	2.5	2	547 (reddish purple)	70 % (2)
8Fe	$CpFe(CO)(PPh_3)$	–	–	–	–	Decomp.
8Ru	$CpRu(CO)(PPh_3)$	58/42	3	3	570 (purple)	>90 % (7)
9Fe	CpFe(dppe)	100/0	–	–	–	–

[a]Isomer ratios at the photostationary states in C_6D_6 determined by ^{1}H NMR

Photochromic behavior of ***M***–DTE is summarized in Table 11.2. It is revealed that the structure of the metal fragments dramatically affected the photochromic properties as observed in dinuclear systems. In the photochromic performance, the mononuclear complexes exhibited lower than the corresponding dinuclear complexes did (Table 11.1).

The mononuclear DTE complexes are also redox-active. CV traces of **9Fe** and **8Ru** apparently contained single reversible redox waves at 450 and 335 mV, respectively. These results suggested that the one-electron redox processes might induce reversible color change of the mononuclear DTE complexes because transition metal fragments can serve as chromophores originated in d–d, MLCT, and LMCT transitions. In fact, radical species $\mathbf{O}^{+\bullet}$ derived from 1e-oxidation of redox-active metal fragments have a characteristic absorption band assigned to LMCT around visible light region (**9Fe**: 676 nm, **8Ru**: 500 nm). As mentioned above, 2e-oxidation of the DTE derivatives with two redox-active organometallic fragments causes the ring closure giving the dicationic closed isomer $\mathbf{C}^{2+}$. That 2e-redox process is not reversible as shown in Figs. 11.7 and 11.8. It is notable, in the mononuclear systems, the color of the open isomer **O** can be changed into two directions in reversible manners (dual chromism), i.e., photochemical ring closure/opening process of DTE moiety between **O** and **C** and 1e-redox process of the organometallic fragment between **O** and $\mathbf{O}^{+\bullet}$ as shown in Fig. 11.12 [68].

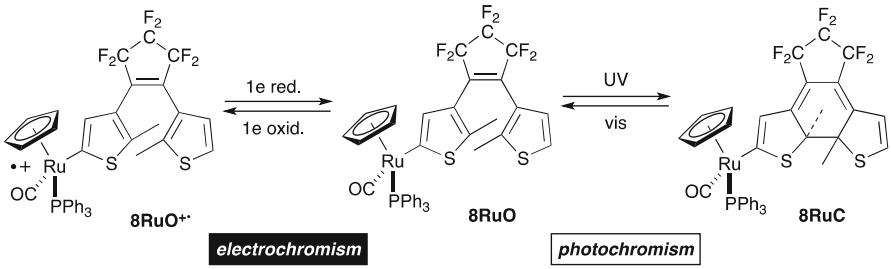

Fig. 11.12 Dual chromism of the mononuclear DTE complexes

These results suggest that combination of a redox-active metal fragment with a DTE makes it dual chromic system (photo- and electrochromism), leading to plural colors and states. Recently, Humphrey and coworkers showed the *multi-stimuli–responsive systems* composed with DTE, redox-active metal fragments, and pH-responsive C≡C units [69]. They have six different states, which can be logically switched by application of the three different stimuli (light, redox, and pH) and detected by a single technique (NLO).

11.4 Conclusion

Photochromic organometallics with a ***M***–C (***M***: redox-active metal fragments, C: carbon atom in the photochromic unit = dithienylethene (DTE)) bond show intriguing stimuli–responsive functions as described above. The functions can lead to molecular devices and sophisticated logic systems.

11.4.1 Molecular Devices

DTE is an excellent switch for π-conjugated systems. Organometallic molecular wires are not also exceptions. Redox properties can be switched photochemically. Switching factors and photochemical process are strongly affected by the structure of metal fragments (Fe or Ru, auxiliary ligands). The basic information on molecular design of metal complexes with photochromic properties has been collected.

11.4.2 Multimodal Stimuli–Responsive Systems

Attachment of a redox-active metal fragment to a photochromic system can make it dual chromic system (photo- and electrochromism). Organic photochromic ligand and redox-active organometallic fragments can serve as photochrome and

electrochrome, respectively. Molecular design is important to construct such stimuli–responsive systems. In particular, the number of metal fragments changes their chromic mechanism. Further combination with other chromic systems and metal fragments should contribute to the development of sophisticated logic systems.

Photochromic organometallics are promising molecular systems for molecular devices and logic systems, although a series of systematic studies is needed for realization. Integration of these stimuli–responsive systems would lead to smart chemical systems.

Acknowledgments This research was financially supported by the Ministry of Education, Culture, Sports, Science and Technology of the Japanese Government (the Grant-in-Aid for Scientific Research on Priority Areas, "New Frontiers in Photochromism (No. 471)" (T.K.), which is gratefully acknowledged. We are also grateful to the Japan Society for Promotion of Science for the Grant-in-Aid for Scientific Research (No. 22350026) (M.A.). We thank Dr Shinichiro Nakamura (RIKEN) for his valuable comments and assistance for computational analysis. A generous gift of perfluorocyclopentene, the starting compound for DTE, from ZEON Corporation is gratefully acknowledged.

References

1. Schwartz M (ed) (2002) Encyclopedia of smart materials. Wiley, New York
2. Bamfield P, Hutchings MG (eds) (2010) Chromic phenomena, technological applications of color chemistry, 2nd ed. Royal Society of Chemistry, Cambridge
3. Irie M (2000) Diarylethenes for memories and switches. Chem Rev 965:1685–1716
4. Irie M, Uchida K (1998) Synthesis and properties of photochromic diarylethenes with heterocyclic aryl groups. Bull Chem Soc Jpn 71:985–996
5. Wang M-S, Xu G, Zhang Z-J, Guo G-C (2010) Inorganic-organic hybrid photochromic material. Chem Commun 46:361–376
6. Tian H, Yang S (2004) Recent progress on diarylethene based photochromic switches. Chem Soc Rev 33:85–97
7. Duerchais V, Le Bozec H (2010) Metal complexes featuring photochromic ligands. Top Organomet Chem 28:171–225 and references therein
8. Ko C-C, Yam VW-W (2010) Transition metal complexes with photochromic ligands-photosensitization and photoswitchable properties. J Mater Chem 20:2063–2070
9. Hasegawa Y, Nakagawa T, Kawai T (2010) Recent progress of luminescent metal complexes with photochromic units. Coord Chem Rev 254:2643–2651
10. Akita M (2011) Photochromic organometallics, a stimuli-responsive system: an approach to smart chemical systems. Organometallics 30:43–51 and references therein
11. Nakai H, Isobe K (2010) Photochromism of organometallic compounds with structural rearrangement. Coord Chem Rev 254:2652–2662 and references therein
12. Jortner J, Ratner M (1997) Molecular electronics. Blackwell, Oxford
13. Aviram A, Ratner M (1998) Molecular electronics: science and technology. Ann N Y Acad Sci
14. Ratner M (2000) Molecular electronics: pushing electrons around. Nature 404:137–138
15. Tour JM (2000) Molecular electronics. Synthesis and testing of components. Acc Chem Res 33:791–804
16. Hipps KW (2001) It's all about contacts. Science 294:536
17. Cahen D, Hodes G (2002) Molecules and electronic materials. Adv Mater 14:789–798
18. Caroll RL, Gorman CB (2002) The genesis of molecular electronics. Angew Chem Int Ed 41:4378–4400

19. Robertson N, McGowan GA (2003) A comparison of potential molecular wires as components for molecular electronics. Chem Soc Rev 32:96–103
20. Reed MA, Lee T (eds) (2003) Molecular nanoelectronics. American Scientific Publishers, Stevenson Ranch
21. Balzani V, Credi A, Venturi M (2003) Molecular devices and machines. Wiley, Weinheim
22. Flood AH, Stoddart JF, Steuerman DW, Heath JR (2004) Where molecular electronics? Science 306:2055–2056
23. Nørgaard K, Bjørnholm T (2005) Supramolecular chemistry on water–towards self-assembling molecular electronic circuitry. Chem Commun 1812–1823
24. Low PJ (2005) Metal complexes in molecular electronics: progress and possibilities. Dalton Trans 2821–2824
25. Benniston AC (2004) Pushing around electrons: towards 2-D and 3-D molecular switches. Chem Soc Rev 33:573–578
26. Schwab PFH, Levin MD, Michl J (1999) Molecular rods. 1. Simple axial rods. Chem Rev 99:1863–1934
27. Schwab PFH, Smith JR, Michl J (2005) Synthesis and properties of molecular rods. 2. Zig–zag rods. Chem Rev 105:1197–1280
28. Zheng QL, Gladysz JA (2005) A synthetic breakthrough into an unanticipated stability regime: readily isolable complexes in which C_{16}–C_{28} polyynediyl chains span two platinum atoms. J Am Chem Soc 127:10508–10509
29. Touchard D, Dixneuf PH (1998) A new class of carbon-rich organometallics. The C_3, C_4 and C_5 metallacumulenes Ru=(C=)$_n$CR$_2$. Coord Chem Rev 178–180:409–429
30. Diederich F, Stang PJ, Tykwinski RR (2004) Acetylene chemistry. Wiley, Weinheim
31. Paul F, Lapinte C (1998) Organometallic molecular wires and other nanoscale-sized devices: an approach using the organoiron (dppe)Cp*Fe building block. Coord Chem Rev 178–180:431–509
32. Ghazala SI, Paul F, Toupet L, Roisnel T, Hapiot P, Lapinte C (2006) Di-organoiron mixed valent complexes featuring "(η^2–dppe)(η^5–Me_5)Fe" endgroups: smooth class-III to class-II transition induced by successive insertion of 1,4-phenylene units in a butadiyne-diyl bridge. J Am Chem Soc 128:2463–2476
33. De Montigny F, Aegrouarch G, Costuas K, Halet J-F, Roisnel T, Toupet L, Lapinte C (2005) Electron transfer and electron exchange between [Cp*(dppe)Fe]n^+ (n = 0, 1) building blocks mediated by the 9,10-bis(ethynyl)anthracene bridge. Organometallics 24:4558–4572
34. Le Narvoir N, Lapinte C (1995) 1,4-Diethynylbenzene bridged Fe(Cp*)(dppe) units: mixed-valence 35-electron and bisiron(III) 34-electron complexes. Organometallics 14:634–639
35. Le Stang S, Paul F, Lapinte C (2000) Molecular wires: synthesis and properties of the new mixed-valence complex [Cp*(dppe)Fe–C≡C–X–C≡C–Fe(dppe)Cp*][PF_6] (X = 2,5–C_4H_2S) and comparison of its properties with those of the related all-carbon-bridged complex (X = –C_4–). Organometallics 19:1035–1043
36. Antonova AB, Bruce MI, Ellis BG, Gaudio M, Humphrey PA, Jevric M, Melino G, Nicholson GK, Perkins GJ, Skelton BW, Stapleton B, White AH, Zaitseva NN (2004) A novel methodology for the synthesis of complexes containing long carbon chains linking metal centres: molecular structures of {Ru(dppe)Cp*}$_2$(μ-C_{14}) and {Co_3(μ-dppm)$(CO)_7$}$_2$(μ_3:μ_3-C_{16}). Chem Commun 960–961
37. Bruce MI, Costuas K, Ellis BG, Halet J-F, Low PJ, Moubaraki B, Murray KS, Ouddai N, Perkins GJ, Skelton BW, White AH (2007) Redox-active complexes containing group 8 metal centers linked by C_2 bridges. Organometallics 26:3735–3745
38. Dembinski R, Bartik T, Bartik B, Jaeger M, Gladysz JA (2000) Toward metal-capped one-dimensional carbon allotropes: wirelike C_6–C_{20} polyynediyl chains that span two redox-active (η^5–Me_5)Re(NO)(PPh_3) endgroups. J Am Chem Soc 122:810–822
39. Stahl J, Mohr W, De Quadras L, Peters TB, Bohling JC, Martín-Alvarez JM, Owen GR, Hampel F, Gladysz JA (2007) sp Carbon chains surrounded by sp^3 carbon double helices: coordination-driven self-assembly of wirelike Pt(C≡C)nPt moieties that are spanned by two P(CH_2)mP linkages. J Am Chem Soc 129:8282–8295

40. De Quadras L, Bauer EB, Mohr W, Bohling JC, Peters TB, Martín-Alvarez JM, Hampel F, Gladysz JA (2007) sp Carbon chains surrounded by sp^3 carbon double helices: directed syntheses of wirelike Pt(C≡C)nPt moieties that are spanned by two P(CH_2)mP linkages via alkene metathesis. J Am Chem Soc 129:8296–8309
41. De Quadras L, Bauer EB, Stahl J, Zhuravlev F, Hampel F, Gladysz JA (2007) sp Carbon chains surrounded by sp^3 carbon double helices: wire-like Pt(C≡C)nPt moieties that are spanned by two α, ω-diphosphines that bear heteroatoms or alkyl substituents. New J Chem 31:1594–1604
42. Akita M, Koike T (2008) Organometallic chemistry of polycarbon species: from clusters to molecular devices. Dalton Trans 3523–3530
43. Tanaka Y, Inagaki A, Akita M (2007) A Photoswitchable molecular wire with the dithienylethene (DTE) linker, (dppe)(η^5–C_5Me_5)Fe–C≡C–DTE–C≡C–Fe(η^5–C_5Me_5)(dppe). Chem Commun 1169–1171
44. Fraysse S, Coudret C, Launay J-P (2000) Synthesis and properties of dinuclear complexes with a photochromic bridge: an intervalence electron transfer switching "On" and "Off". Eur J Inorg Chem 1581–1590
45. Tanaka Y, Ishisaka T, Inagaki A, Koike T, Lapinte C, Akita M (2010) Photochromic organometallics with a dithienylethene (DTE) bridge, [Y–C≡C–DTE–C≡C–Y] (Y={MCp*(dppe)}): photoswitchable molecular wire (M=Fe) versus dual photo- and electrochromism (M=Ru). Chem Eur J 16:4762–4776
46. Irie M, Lifka T, Kobatake S, Kato N (2000) Photochromism of 1,2-bis(2-methyl-5-phenyl-3-thienyl)perfluorocyclopentene in a single-crystalline phase. J Am Chem Soc 122:4871–4876
47. Motoyama K, Koike T, Akita M (2008) Remarkable switching behavior of bimodally stimuli-responsive photochromic dithienylethenes with redox-active organometallic attachments. Chem Commun 5812–5814
48. Motoyama K, Li H, Koike T, Hatakeyama M, Yokojima S, Nakamura S, Akita M (2011) Photo- and electro-chromic organometallics with dithienylethene (DTE) linker, L_2CpM-DTE-MCpL_2: dually stimuli-responsive molecular switch. Dalton Trans 40:10643–10657
49. Petz W (1992) Iron–carbene complexes. Springer, Berlin
50. Brookhart M, Studabaker WB (1987) Cyclopropanes from reactions of transition metal carbene complexes with olefins. Chem Rev 87:411–432
51. Liu YF, Lagrost C, Constuas K, Touchar N, Le Bozac H, Rigaut S (2008) A multifunctional organometallic switch with carbon-rich ruthenium and diarylethene units. Chem Commun 6117–6118
52. Lin Y, Yuan JJ, Hu M, Yin J, Jin S, Liu SH (2009) Syntheses and properties of binuclear ruthenium vinyl complexes with dithienylethene units as multifunction switches. Organometallics 28:6402–6409
53. Kawai SH, Gilat SL, Ponsinet R, Lehn J-M (1995) A dual-mode molecular switching device: bisphenolic diarylethenes with integrated photochromic and electrochromic properties. Chem Eur J 1:285–293
54. Koshido T, Kawai T, Yoshino K (1995) Optical and electrochemical properties of cis-1,2-dicyano-1,2-bis(2,4,5-trimethyl-3-thienyl)ethane. J Phys Chem 99:6110–6114
55. Peters A, Branda NR (2003) Electrochromism in photochromic dithienylcyclopentenes. J Am Chem Soc 125:3404–3405
56. Peters A, Branda NR (2003) Electrochemically induced ring-closing of photochromic 1,2-dithienylcyclopentenes. Chem Commun 954–955
57. Zhou X-H, Zhang F-S, Yuan P, Sun F, Pu S-Z, Zhao F-Q et al (2004) Photoelectrochromic dithienylperfluorocyclopentene derivatives. Chem Lett 33:1006–1007
58. Moriyama Y, Matsuda K, Tanifuji N, Irie S, Irie M (2005) Electrochemical cyclization/cycloreversion reactions of diarylethenes. Org Lett 7:3315–3318
59. Guirado G, Coudret C, Hliwa M, Launay J-P (2005) Understanding electrochromic processes initiated by dithienylcyclopentene cation-radicals. J Phys Chem B 109:17445–17459

60. Grabom T, Petersilka M, Gross EKU (2000) Molecular excitation energies from time-dependent density functional theory. THEOCHEM 501:353–367
61. Furche F (2001) On the density matrix based approach to time-dependent density functional response theory. J Chem Phys 114:5982–5992
62. Becke AD (1993) Density functional thermochemistry. III. The role of exact exchange. J Chem Phys 98:5648–5652
63. Lee C, Yang W, Parr RG (1998) Development of the colle-salvetti correlation-energy formula into a functional of the electron density. Phys Rev B 37:785–789
64. Hania PR, Telesca R, Lucas LN, Pugzlys A, Van Esch J, Feringa BL, Snijders JG, Duppen K (2002) An optical and theoretical investigation of the ultrafast dynamics of a bisthienylethene-based photochromic switch. J Phys Chem A 106:8498–8507
65. Guillaumont D, Kobayashi T, Kanda K, Miyasaka H, Uchida K, Kobatake S, Shibata K, Nakamura S, Irie M (2002) An ab Initio MO study of the photochromic reaction of dithienylethenes. J Phys Chem A 106:7222–7227
66. Jukes RTF, Adamo V, Hartl F, Belser P, De Cola L (2004) Photochromic dithienylethene derivatives containing Ru(II) or Os(II) metal units. Sensitized photocyclization from a triplet state. Inorg Chem 43:2779–2792
67. Hatakeyama M, Yokojima S, Shinoda K, Koike T, Akita M, Nakamura S (2012) Theoretical study on the photocyclization mechanism of diarylethenes with transition-metal substituents. Bull Chem Soc Jpn 85:679–686
68. Li H, Koike T, Akita M (2012) Color change of redox-active organometallic dithienylethene complexes by photochemical and redox processes. Dyes Pigm 92:854–860
69. Green KA, Cifuentes MP, Corkery TC, Samoc M, Humphrey MG (2009) Switching the cubic nonlinear optical properties of an electro-, halo-, and photochromic ruthenium alkynyl complex across six states. Angew Chem Int Ed 48:7867–7870